Asian Journal of Chemistry; Vol. 30, No. 8 (2018), 1815-1822

ASIAN JOURNAL OF CHEMISTRY

https://doi.org/10.14233/ajchem.2018.21323

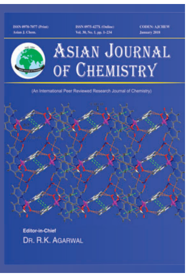

Synergistic Influence of Halide Ions on Corrosion Inhibition Performance of Gum Exudates of *Azadirachta indica* on Carbon Steel in Sulphuric Acid Medium

MALARVIZHI MANICKAM[1,*], DHEENADHAYALAN SIVAKUMAR[2] and MALLIKA JAGANATHAN[2]

[1]Department of Chemistry, Sri GVG Visalakshi College for Women, Udumalpet-642 128, India
[2]Department of Chemistry, PSG College of Arts and Science, Coimbatore-641 014, India

*Corresponding author: E-mail: malar_gvg@rediffmail.com

Received: 7 March 2018; *Accepted*: 17 May 2018; *Published online*: 30 June 2018; AJC-18980

The effect of halide ions on the inhibitive performance of gum exudates of *Azadirachta indica* on carbon steel in 1 N sulphuric acid medium was investigated using chemical and electrochemical methods. Effect of temperature and immersion period on mitigation performance was studied. The inhibition efficiency of gum exudates of *Azadirachta indica* considerably increased with the presence of halide ions at all temperature ranges studied. Synergistic influence of halide ions on gum exudates of *Azadirachta indica* for carbon steel corrosion was reported. Adsorption of gum exudates of *Azadirachta indica* as well as the inhibitor mixtures are spontaneous and the process followed Langmuir adsorption isotherm. SEM studies supported the adsorption phenomenon.

Keywords: *Azadirachta indica* gum, Corrosion inhibitor, Electrochemical studies, Synergistic effect, Halide ions.

INTRODUCTION

Carbon steel finds extensive use in oil refineries, distillation plants petrochemical industries, power plants, gas refineries and ships due to its high strength, low cost and easy accessibility [1]. Nevertheless, a huge problem towards application part of carbon steel is its corrosion especially in acid media. Steel corrosion in acidic medium can be minimized through several approaches. Use of synthetic organic and inorganic compounds as corrosion inhibitors is the well-established method but is much expensive and non-biodegradable. To prevail with the condition, bountiful number of corrosion research studies were done using extracts of different parts of plants, natural products, drugs and biopolymers.

Some investigations of gum exudates of trees reported as good inhibitors made in the recent past include gum arabic [2], locust bean gum [3], guar gum [4], albizia gum [5], *Raphia hookeri* exudate gum [6], *Dacryodes edulis* gum [7], *Ficus glumosa* gum [8], *Commiphora kerstingii* gum [9], *Ficus benjamina* gum [10], *Anogeissus leiocarpus* gum [11], *Commiphora penndunculata* gum [12], *Ficus platyphylla* gum [13], *Ficus trichopoda* gum [14], *Gloriosa superba* gum [15], *Khaya ivorensis* gum [16], *Ficus thonningii* gum [17] and *Daniella oliveri* gum [18]. In general, to improve efficiency of naturally occurring substances, a small addition of halide ions are employed [19-21]. We had reported earlier the use of *Azadirachta indica* gum for mild steel corrosion in hydrochloric acid medium [22]. The current research work is focused on the impact made by halide ions in gum exudates of *Azadirachta indica* (GAI) performance for corrosion control of carbon steel in sulphuric acid medium. Gravimetric methods and electrochemical methods were made used to obtain the inhibition efficiency of GAI and surface morphological studies were carried out by using SEM studies.

Gum exudate of *Azadirachta indica* is basically a salt of complex polysaccharide which is obtained from *Melia azadirachta* [23]. Anderson and Hendrie [24] reported that neem gum contains:

- 35 % of proteinaceous material which is mostly made of mainly serine, threonine and aspartic acid.
- A very complex carbohydrate component which constitutes D-glucose, D-glucoronic acid, arabinose, fucose, mannose, xylose, rhamnose, D-glucosamine, D-galactose and aldobiuronic acid.

From the above facts, it can be ascribed that GAI with its larger size, typical hetero atoms and sensitive functional groups could adsorb onto the metal surface in an extensive manner subsequently reducing the corrosion rate.

EXPERIMENTAL

Metal specimen: Rectangular shaped carbon steel specimens with a dimension of 25 mm × 10 mm × 1 mm were used to carry out the gravimetric experiments. The composition of the coupon was (in wt %) 0.68 % Mn, 0.37 % C, 0.23 % Si, 0.16

% Cu, 0.077 % Cr, 0.0059 % Ni, 0.016 % S, 0.011 % Ti, 0.009 % Co (in wt. %), rest being Fe. Prior to experiments, each coupon was polished by 100, 400 and 600 grades of emery sheet, washed with ethanol, cleaned with acetone and dried, stored in desiccator. Double distilled water was used to prepare aggressive medium of analytical grade sulphuric acid. For synergistic studies AnalaR grade potassium salts were used.

Preparation of gum exudate inhibitor: Gum exudates of *Azadirachta indica* collected locally was dissolved in water and filtered to remove the impurities. The filtrate was then dried to obtain solid GAI, which is found soluble in water.

Methods: The chemical method was carried out as per ASTM [25] standard and electrochemical methods were carried out as previously reported [22]. The surface of the inhibited and uninhibited carbon steel surface was analyzed by SEM studies.

RESULTS AND DISCUSSION

Weight loss measurements: The corrosion behaviour of carbon steel in the absence and presence of various concentrations of GAI and GAI in combination with halide ions was investigated using weight loss measurements in the temperature range of 303 to 323 K for 1 and 4 h immersion period. Corrosion rate, inhibition efficiency and surface area were calculated with the following expressions:

$$\text{Corrosion rate (CR) (mmpy)} = 87.6 \times \frac{W}{\rho A t} \quad (1)$$

$$\text{Inhibition efficiency (IE) (\%)} = \frac{W_o - W_i}{W_o} \times 100 \quad (2)$$

$$\text{Surface coverage } (\theta) = 1 - \frac{W_i}{W_o} \quad (3)$$

where W is the weight loss, ρ density of carbon steel, A is the exposed surface area and t is the immersion time. Also W_i and W_o are weight loss of carbon steel in the presence and absence of GAI. The corrosion parameters were presented in the Tables 1 and 2. Close inspection of Table-1 shows that with increase in concentration corrosion rate decreases but increases with increase in temperature. It is attributed to dissolution of carbon steel as well as desorption of adsorbed inhibitor increases with increase in temperature. Such a behaviour is ideal for chemical mode of adsorption. Assessment and comparison of Tables 1 and 2 reveal that the rate of corrosion decreased for the solutions containing GAI and GAI + halide ions compared to the blank solution.60 ppm GAI at 303 K shows an inhibition efficiency of 68.75 % whereas in combination with 1 mM of KI, efficiency is boosted up to 95.31 % for 1h immersion time. While in the case of 4 h immersion time, inhibition efficiency shown by GAI and GAI + KI mixture is found to be 85.20 and 95.40 % respectively.

To analyze the inhibitor adsorption mechanism in terms of activation energy E_a^*, Arrhenius equation (eqn. 4) related to frequency factor A is used.

$$\log CR = \log A - \frac{E_a^*}{2.303RT} \quad (4)$$

Graphs between log CR and 1/T for different concentrations of GAI in addition with halide ions plotted were presented in Figs. 1a-c and 2a-c for 1 h and 4 h immersion periods. This linear regression plots gave straight line with slope $-E_a^*/2.303$ R from which activation energy was obtained.

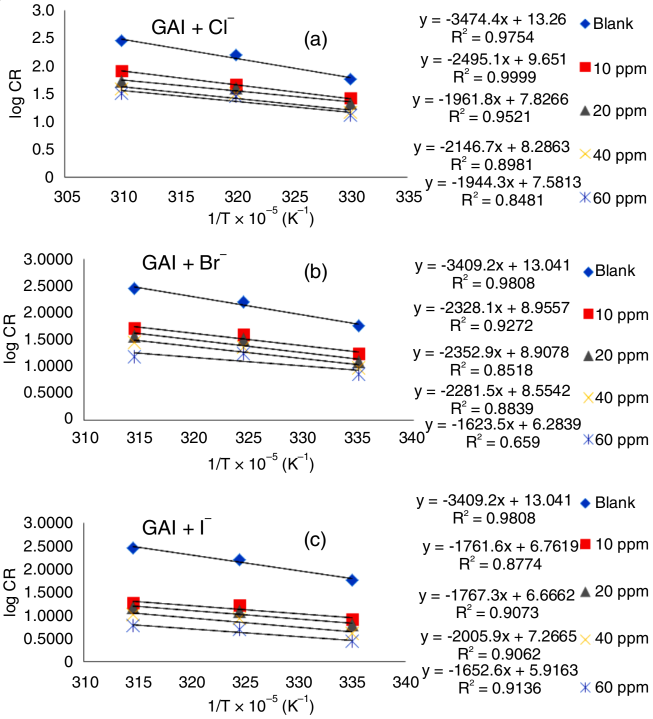

Fig. 1a-c. Arrhenius plots for GAI + X^- ion mixture on carbon steel in 1 N H_2SO_4 for 1 h immersion period

TABLE-1
CORROSION PARAMETERS OBTAINED FROM WEIGHT LOSS MEASUREMENTS FOR CARBON STEEL IN 1N H_2SO_4 CONTAINING VARIOUS CONCENTRATIONS OF GAI AT DIFFERENT TEMPERATURES

Immersion period (h)	[GAI] (ppm)	303 K			313 K			323 K		
		Corrosion rate (mmpy)	Inhibition efficiency (%)	Surface coverage (θ)	Corrosion rate (mmpy)	Inhibition efficiency (%)	Surface coverage (θ)	Corrosion rate (mmpy)	Inhibition efficiency (%)	Surface coverage (θ)
1	Blank	57.8620	–	–	160.4767	–	–	277.5569	–	–
	10	27.5749	52.34	0.5234	78.6562	50.99	0.5099	91.7656	66.94	0.6694
	20	23.9585	58.59	0.5859	56.5059	64.79	0.6479	63.2866	77.20	0.7720
	40	19.8901	65.63	0.6563	38.4240	76.06	0.7606	49.2731	82.25	0.8225
	60	18.0819	68.75	0.6875	33.9035	78.87	0.7887	45.2047	83.71	0.8371
4	Blank	56.5165	–	–	221.0556	–	–	361.8612	–	–
	10	12.8843	77.20	0.7720	124.2078	43.81	0.4381	226.3656	37.45	0.3745
	20	11.3078	80.00	0.8000	99.5634	54.96	0.5496	209.3024	42.16	0.4216
	40	9.8334	82.60	0.8260	69.9512	68.35	0.6835	166.8142	53.90	0.5390
	60	8.3656	85.20	0.8520	64.0210	71.04	0.7104	135.5016	62.55	0.6255

TABLE-2
CORROSION PARAMETERS OBTAINED FROM WEIGHT LOSS MEASUREMENTS FOR CARBON STEEL IN 1 N H_2SO_4 CONTAINING VARIOUS GAI CONCENTRATIONS IN COMBINATION WITH HALIDE IONS AT DIFFERENT TEMPERATURES

Immersion period (h)	Concentration		303 K			313 K			323 K		
	X^- (1 mM)	GAI (ppm)	Corrosion rate (mmpy)	Inhibition efficiency (%)	Surface coverage (θ)	Corrosion rate (mmpy)	Inhibition efficiency (%)	Surface coverage (θ)	Corrosion rate (mmpy)	Inhibition efficiency (%)	Surface coverage (θ)
1	Cl^-	10	26.22	54.69	0.5469	46.11	71.27	0.7127	82.72	70.20	0.7020
		20	21.25	63.28	0.6328	39.78	75.21	0.7521	52.44	81.11	0.8111
		40	14.47	75.00	0.7500	31.64	80.28	0.8028	38.88	85.99	0.8599
		60	13.11	77.34	0.7734	28.48	82.25	0.8225	32.10	88.44	0.8844
	Br^-	10	17.18	70.31	0.7031	39.33	75.49	0.7549	51.08	81.60	0.8160
		20	12.21	78.91	0.7891	32.10	80.00	0.8000	36.62	86.81	0.8681
		40	9.49	83.59	0.8359	23.05	85.63	0.8563	27.57	90.07	0.9007
		60	7.23	87.50	0.8750	17.18	89.30	0.8930	15.37	94.46	0.9446
	I^-	10	8.13	85.94	0.8594	16.27	89.86	0.8364	18.53	93.53	0.9124
		20	6.32	89.06	0.8906	12.20	92.39	0.8773	14.46	94.95	0.9316
		40	4.06	92.97	0.9297	8.58	94.65	0.9136	10.39	96.37	0.9509
		60	2.71	95.31	0.9531	4.97	96.90	0.9500	5.87	97.95	0.9722
4	Cl^-	10	11.41	79.80	0.7980	68.94	68.81	0.6881	122.84	66.05	0.6605
		20	9.95	82.40	0.8240	54.36	75.41	0.7541	107.59	70.27	0.7027
		40	8.70	84.60	0.8460	36.05	83.69	0.8369	87.70	75.77	0.7577
		60	7.23	87.20	0.8720	32.21	85.43	0.8543	69.95	80.67	0.8067
	Br^-	10	10.06	82.20	0.8220	63.29	71.37	0.7137	114.93	68.24	0.6824
		20	8.36	85.20	0.8520	48.71	77.97	0.7797	104.20	71.21	0.7121
		40	7.80	86.20	0.8620	32.66	85.22	0.8522	80.92	77.64	0.7764
		60	6.44	88.60	0.8860	27.69	87.47	0.8747	64.30	82.23	0.8223
	I^-	10	8.93	84.20	0.8420	55.38	74.95	0.7495	123.18	65.96	0.6596
		20	7.23	87.20	0.8720	44.19	80.01	0.8001	98.55	72.77	0.7277
		40	6.67	88.20	0.8820	32.66	85.22	0.8522	79.90	77.92	0.7792
		60	5.31	90.60	0.9060	24.30	89.01	0.8901	55.26	84.73	0.8473

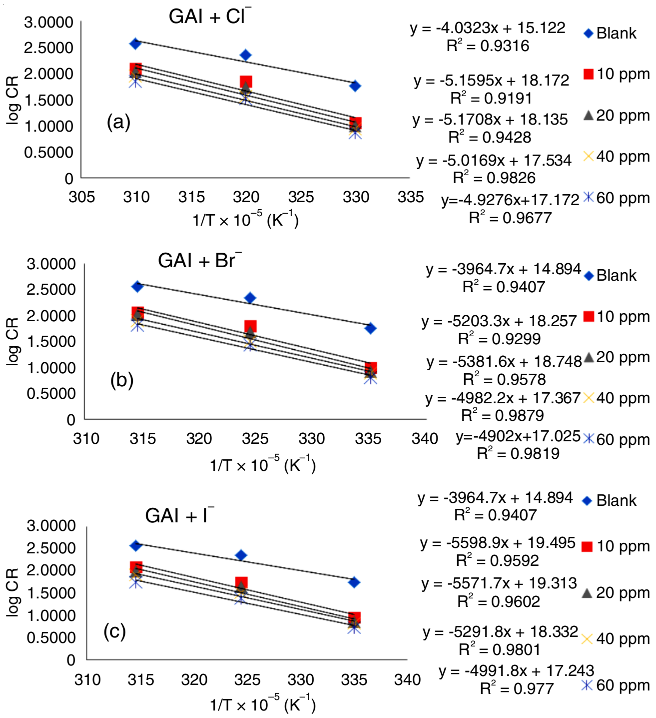

Fig. 2a-c. Arrhenius plots for GAI + X⁻ ion mixture on carbon steel in 1 N H_2SO_4 for 4 h immersion period

Eqn. 5, the alternative form of Arrhenius equation is used to attain the enthalpy and entropy of corrosion process.

$$CR = \left(\frac{RT}{Nh}\right)\exp\left(\frac{\Delta S^*}{R}\right)\exp\left(\frac{-\Delta H^*}{RT}\right) \quad (5)$$

Figs. 3a-c and 4a-c shows the plots of CR/T *vs.* 1/T for immersion periods 1h and 4h.These graphs gave straight line with slope ($-\Delta H^*/2.303R$) and an intercept (log (R/Nh) + $\Delta S^*/$

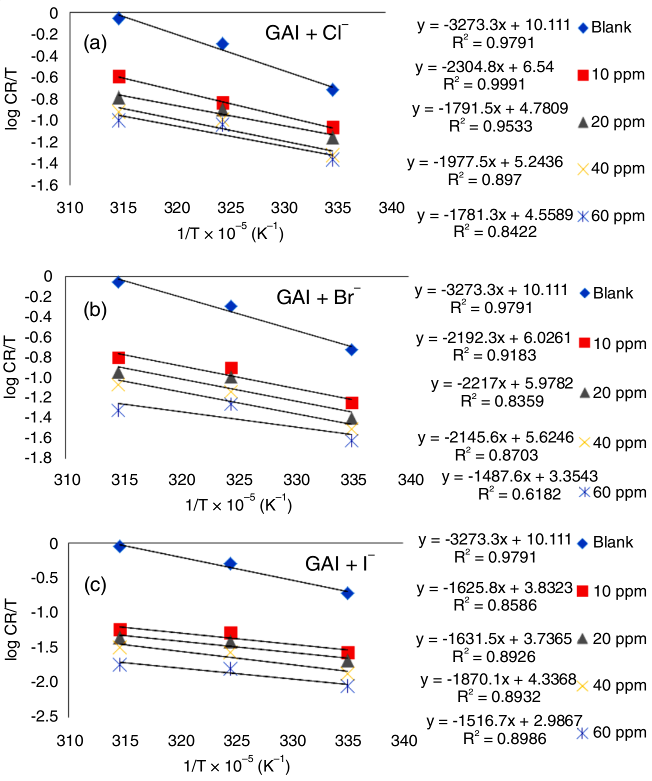

Fig. 3a-c. Transition plots for GAI + X⁻ ion mixture on carbon steel in 1 N H_2SO_4 for 1 h immersion period

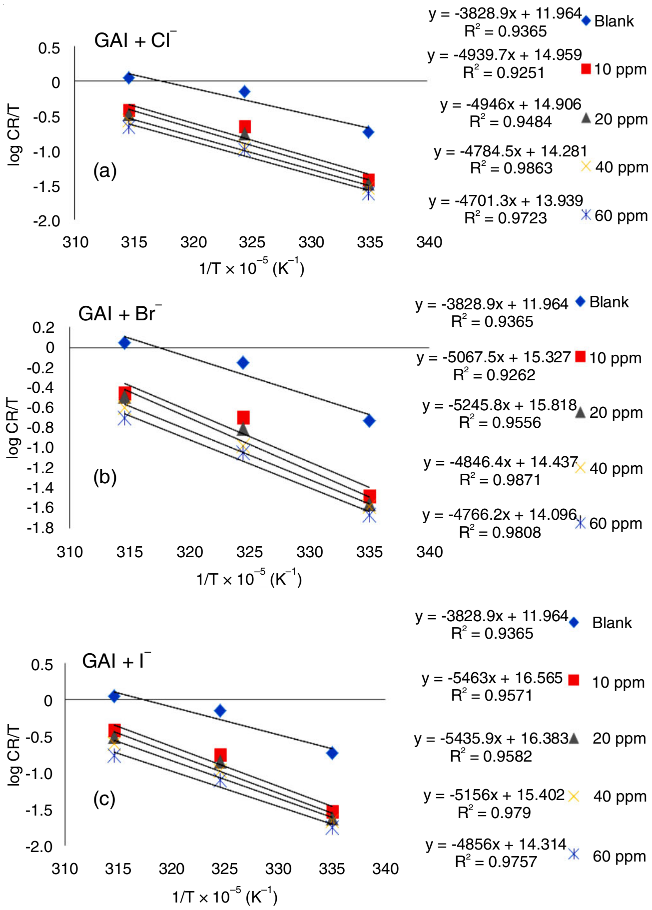

Fig. 4a-c. Transition plots for GAI + X⁻ ion mixture on carbon steel in 1 N H_2SO_4 for 4 h immersion period

2.303 R), from which enthalpy (ΔH*) and entropy (ΔS*) of activation was obtained and those values were presented in Table-3.

Analysis of Table-3 indicates that activation energy is lower in inhibited solutions than in uninhibited solutions. This decrease in E_a value on addition of GAI-halide combination was ascribed to their chemisorption on carbon steel surface [26,27]. Enthalpy change (ΔH*) in presence of GAI-halide mixture found lesser compared to blank than the blank again established the chemical mode of adsorption. In addition, change in enthalpy values being positive reflects the endothermic nature of the corrosion process [28,29]. The values of ΔS* for the uninhibited solution decreases towards more negative side with increase in concentration of GAI in the inhibitor system which depicts the increase in disorder as there would be conversion of reactants into activated complexes [30]. The calculated E_a, ΔH* and ΔS values of the inhibitor mixtures for 4 h immersion time are presented in the Table-3. In contrast, for 4 h immersion period, the results obtained validate the physical mode of adsorption.

Adsorption isotherm gives information about inhibitor adsorption on the surface [31,32]. Various kinds of isotherms such as Langmuir, Frumkin, Freundlich, El-Awady and Temkin were tried for both 1 h and 4 h immersion time and Langmuir is found to be the best fit isotherm. Figs. 5a-c shows the Langmuir plots for 1 h immersion time. Accordingly concentration (C), equilibrium constant (K_{ads}) and surface coverage (θ) is related as:

$$C/\theta = 1/K_{ads} + C \qquad (6)$$

Correlation coefficient values ($R^2 > 0.99$) were suggestive of the phenomenon that the adsoption process obeyed

TABLE-3
ACTIVATION PARAMETERS OBTAINED FROM WEIGHT LOSS MEASUREMENTS FOR CARBON STEEL IN 1 N H_2SO_4 SOLUTION CONTAINING VARIOUS CONCENTRATIONS OF GAI IN THE PRESENCE OF HALIDE IONS

Immersion period (h)	Halide ion concentration (1 mM)	Concentration of GAI (ppm)	E_a (kJ mol^{-1})	ΔH (kJ mol^{-1})	ΔS (J K^{-1} mol^{-1})	E_a-ΔH
1		Blank	66.5247	63.8671	-11.292	2.6
	Cl⁻	10	47.7743	45.1167	-80.389	2.6
		20	37.5628	34.9052	-115.322	2.6
		40	41.1039	38.4463	-106.520	2.6
		60	37.2278	34.5702	-120.020	2.6
	Br⁻	10	45.3112	42.6536	-91.220	2.6
		20	45.6775	43.019	-92.481	2.6
		40	44.3362	41.6786	-99.173	2.6
		60	31.3399	28.6823	-143.951	2.6
	I⁻	10	34.2266	31.5689	-134.019	2.6
		20	34.3712	31.7136	-135.737	2.6
		40	39.0109	36.3532	-124.004	2.6
		60	32.1473	29.4896	-150.188	2.6
4		Blank	77.2061	74.5485	24.356	2.6
	Cl⁻	10	98.7904	96.1328	82.767	2.6
		20	99.00549	96.3478	82.047	2.6
		40	96.0584	93.4008	70.542	2.6
		60	94.34854	91.6909	63.619	2.6
	Br⁻	10	101.2818	98.6241	89.967	2.6
		20	104.8784	102.2208	99.967	2.6
		40	97.2736	94.6159	73.629	2.6
		60	95.6627	93.0050	66.850	2.6
	I⁻	10	109.1195	106.4619	114.540	2.6
		20	108.5965	105.9389	111.039	2.6
		40	103.2574	100.5998	92.309	2.6
		60	97.38342	94.7258	71.040	2.6

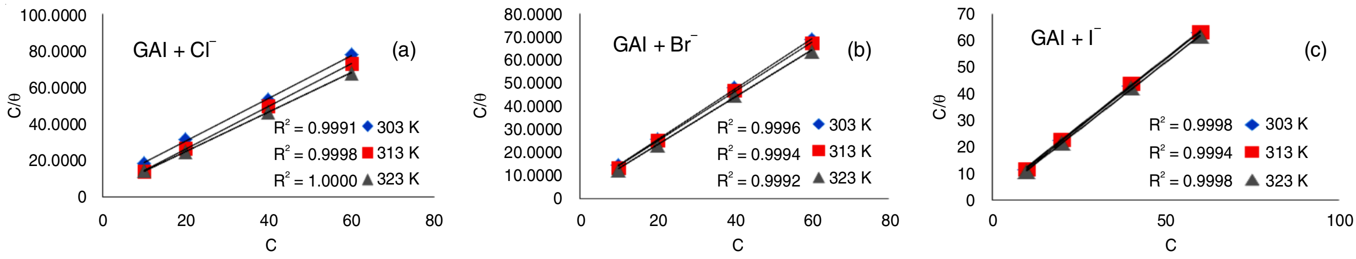

Fig. 5a-c. Langmuir adsorption isotherm plots for GAI with halide ions for 1 h immersion period

Langmuir model. Equilibrium constant and free energy of adsorption($\Delta G°$) is related as:

$$K = -\log C_{H_2O} - \left(\frac{\Delta G^o_{ads}}{2.303RT}\right) \qquad (7)$$

The negative ΔG^o_{ads} shown in the Table-4 indicates that a spontaneous adsorption of GAI + halide ion mixture took place with strong interaction on carbon steel surface [33]. Investigation of the experimental results indicates that the inhibitor system adsorbed chemically for 1 h immersion time and physically for 4 h immersion time.

Synergistic effect: Synergistic corrosion inhibition is a proficient approach to enhance the performance ability of inhibitors in terms of quantity and varied utility. The combined action of compounds in total giving higher effect than the individual effect is called synergistic inhibition effect. Synergistic studies of organic compounds with halides have been extensively studied [21,34-36]. Addition of halides to corrosive media enhances the adsorption capacity of the inhibitors by bridging between inhibitor cations and negatively charged metal surface. Synergistic effect using iodide ion excelled compared to that of chloride and bromide ions. This is attributed to the fact that iodide ions has ionic radius, polarizability and hydrophobicity higher than bromide and chloride ions [37,38].

Determination of extent of synergistic influence *i.e.* synergism parameter can be obtained from eqn. 8:

$$S = \frac{1-(\eta_1+\eta_2)}{1-\eta_{1+2}} \qquad (8)$$

where η_1, η_2 are the inhibition efficiencies of GAI and halide ions respectively and η_{1+2} is the combined efficiency of the inhibitor mixtures.

Addition of halide ion with GAI showed very high inhibition efficiency than that in the absence of halides. This reflects that there was synergism exhibiting between the halide ions and GAI in 1 N sulphuric acid medium for carbon steel corrosion control from which it was understood that strong chemical adsorption of halide ions on carbon steel surface [39]. When the halide ions get into the double layer of the metallic substrate, the charge of the halide befits the charge of the carbon steel surface [40,41]. So coulombic attraction plays the role in adsorption process. On stabilization of adsorbed halide ions, better surface coverage is possible so that greater inhibition performance is effected [42]. The synergistic mechanism may be either competitive or cooperative [43]. Competitive adsorption is one where cations of the inhibitor is adsorbed at various metal sites while in co-operative adsorption anions are chemisorbed on metal substrate and the cations on anion layers. There are some cases where both mechanisms operate occur simultaneously [19]. Generally, S < 1 denotes antagonistic effect while S > 1 denotes synergistic behaviour [44]. Most of the values of S > 1 presented in Table-5 reveals that there pre vailed synergism between GAI and halide ions for carbon steel corrosion control in sulphuric acid. Some values S < 1 is also observed.

Potentiodynamic polarization studies: Anodic and cathodic polarization curves with and without inhibitor for

TABLE-4
LANGMUIR ADSORPTION PARAMETERS FOR MILD STEEL CORROSION IN H_2SO_4
CONTAINING VARIOUS CONCENTRATIONS OF GAI IN PRESENCE OF 1 mM of X^- IONS

Immersion period (h)	X^- (1 mM)	Temperature (K)	R^2	Slope	ΔG_{ads} (kJ/mol)
1	Cl^-	303	0.999	1.1707	-34.1700
		313	0.999	1.1739	-37.8300
		323	1.000	1.0751	-38.4400
	Br^-	303	0.999	1.0900	-35.9200
		313	0.999	1.0763	-36.3100
		323	0.999	1.0278	-36.9200
	I^-	303	0.999	1.0246	-37.9030
		313	0.999	1.0245	-37.1270
		323	0.999	1.0154	-38.9730
4	Cl^-	303	0.999	1.1264	-20.5158
		313	0.999	1.1060	-18.9482
		323	0.999	1.1830	-19.2732
	Br^-	303	0.999	1.1140	-21.1900
		313	0.999	1.0863	-19.1900
		323	0.999	1.1608	-19.3800
	I^-	303	0.999	1.0898	-21.3100
		313	0.999	1.0801	-19.5200
		323	0.999	1.1171	-18.8900

TABLE-5
SYNERGISTIC PARAMETERS FOR DIFFERENT CONCENTRATIONS OF GAI WITH 1 mM OF HALIDE IONS

Immersion period (h)	Concentration		Synergistic parameter		
	X^- (1 mM)	GAI (ppm)	303 K	313 K	323 K
1	Cl^-	10	1.51	1.17	1.01
		20	1.40	1.20	1.00
		40	1.27	1.18	1.01
		60	1.28	1.15	0.99
	Br^-	10	1.59	0.88	1.31
		20	1.49	1.00	1.35
		40	1.49	1.07	1.36
		60	1.46	1.06	1.31
	I^-	10	1.53	1.01	1.36
		20	1.55	1.14	1.45
		40	1.56	1.23	1.48
		60	1.56	1.23	1.47
4	Cl^-	10	1.03	0.97	1.02
		20	1.03	1.03	1.03
		40	1.03	1.09	1.11
		60	1.03	1.10	1.15
	Br^-	10	1.16	1.12	1.07
		20	1.15	1.17	1.07
		40	1.15	1.21	1.15
		60	1.15	1.22	1.19
	I^-	10	1.19	0.99	0.93
		20	1.18	1.08	0.97
		40	1.16	1.20	1.08
		60	1.16	1.20	1.15

carbon steel in 1N sulphuric acid solution were depicted in Fig. 6. These curves on extrapolation was used to obtain corrosion current density and corrosion potential. Using corrosion current density with (i_{corr}) and without (i°_{corr}) the inhibitor, efficiency of the inhibitor can be calculated using eqn. 9:

$$\text{Inhibition efficiency} = \frac{i^{o}_{corr} - i_{corr}}{i_{corr}} \times 100 \qquad (9)$$

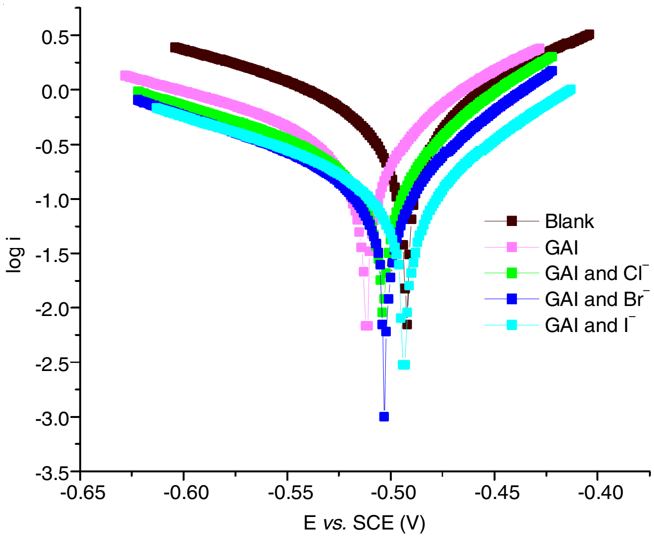

Fig. 6. Potentiodynamic polarization curves for carbon steel in the absence and presence of inhibitor mixtures

The inhibition efficiency calculated using expression (eqn. 9), the electrochemical polarization factors E_{corr}, I_{corr}, anodic and cathodic tafel slopes were listed in Table-6. Fig. 6 reflects that upon the addition of GAI and GAI + halide mixture to 1 N H_2SO_4 solution, slope of both anodic and cathodic curves changed. The results obtained depicted the impedance in hydrogen evolution at the cathode and metal dissolution at the anode. So it could be understood that GAI and GAI-halide mixture affected cathodic as well as anodic reactions. Table-6 shows that the presence of inhibitors reduces the corrosion current density indicating that inhibitor get absorbed onto the metal surface. Since there is not much change in the nature of the polarization curves, it was assumed that the inhibitor system hinder the deterioration reaction through the same mechanism. A small change in the value of E_{corr} in comparison with and without inhibitor indicated the mixed mode type of inhibitor [45]. The maximum difference was found to be 23 mV, which indicates that the inhibitors possibly will be of mixed type [46,47]. This fact is supported by the behaviour of Tafel slopes b_a and b_c also. Addition of halide ions to GAI decreased the corrosion current thereby increasing the inhibitor efficiency. In particular addition of iodide ions decrease the I_{corr} value from 410 to 103 mA/cm^2 owing to its strong chemical adsorption increasing the mitigation performance in aggressive solution [48]. The following order of inhibitor mixture performance is observed:

GAI + KI > GAI + KBr > GAI + KCl

TABLE-6
ELECTROCHEMICAL POLARIZATION PARAMETERS FOR CARBON STEEL IN 1 N H_2SO_4 IN THE ABSENCE AND PRESENCE OF 60 ppm GAI AND 1 mM HALIDE MIXTURES

Concentration (ppm)	$-E_{corr}$ (V *vs.* SCE)	I_{corr} (mA/ cm^2)	Tafel slope (mV/decade)		Inhibition efficiency (%)
			b_a	b_c	
Blank	490.1	410	85	137	–
GAI	513.6	201	74	160	55.60
GAI + Cl^- ion	496.3	164	64	154	60.00
GAI + Br^- ion	495.5	114	62	143	72.19
GAI + I^- ion	485.7	103	69	149	74.87

Electrochemical impedance measurements: Fig. 7 shows the Nyquist plots from which the impedance data for carbon steel in 1N sulphuric acid without, with 60 ppm GAI in the presence and absence of halide ions in the presence and absence of halide ions was given in Table-7. Data describes the single, depressed semicircles shows presence of GAI and GAI-mixture was not affecting the corrosion mechanism process and in addition the charge transfer process undertakes completely the corrosion process [49]. Using charge transfer values with (R_{ct}) and without (R°_{ct}) inhibitor, inhibition efficiency was calculated as follows:

$$\text{Inhibition efficiency} = \frac{R_{ct} - R^{o}_{ct}}{R_{ct}} \times 100 \qquad (10)$$

Inhibition efficiency obtained from eqn. 10, charge transfer resistance and double layer capacitance were shown in the Table-7. The double layer capacitance (C_{dl}) can be calculated from the expression (eqn. 11) which is related to charge transfer resistance and frequency f_{max} as:

$$C_{dl} = 1/2\, \pi\, f_{max}\, R_{ct} \qquad (11)$$

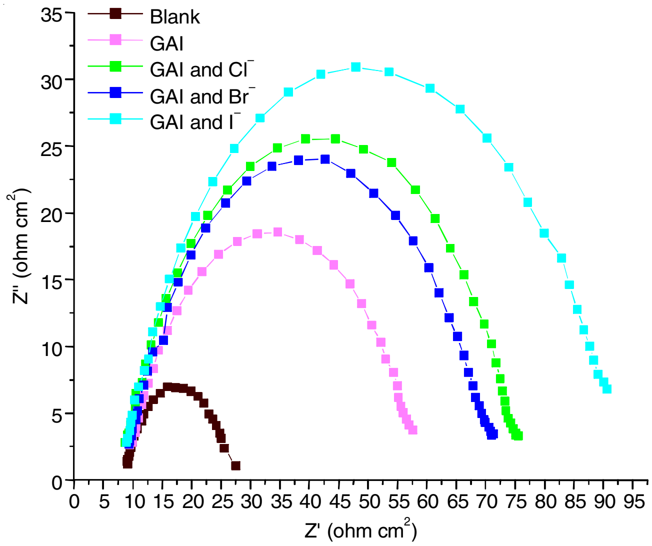

Fig. 7. Nyquist plots for carbon steel in the absence and presence of inhibitor mixtures

TABLE-7
AC IMPEDANCE PARAMETERS FOR CARBON STEEL IN 1 N H_2SO_4 IN THE ABSENCE AND PRESENCE OF 60 ppm GAI AND 1 mM HALIDE MIXTURES

Concentration (ppm)	R_{ct} (Ω cm^{-2})	C_{dl} (μF cm^{-2}) $\times 10^{-3}$	Inhibition efficiency (%)
Blank	19.19	35.1	–
60 ppm GAI	48.4	14.1	60.35
GAI + Cl^- ion	51.2	13.9	62.51
GAI + Br^- ion	68.8	13.2	72.10
GAI + I^- ion	89.5	12.3	78.56

Actually R_{ct} is a measure of electron transfer and it can be seen that R_{ct} value increased considerably for test solutions containing halide ions along with the inhibitor owing to the development of thin film of protective layer at the metal-solution interface [50]. In general, the double layer formed was considered like capacitor, where in presence of inhibitor the electrical capacity of the double layer decreases. This may be due to the displacement of water molecules and other adsorbed molecules. This fact leads to the formation of insulating protective layer which increases the thickness of the double layer. From the Table-7, it can be found that the C_{dl} value of uninhibited solution is higher compared to inhibited solutions. Addition of GAI lowers the C_{dl} from 35.1× 10^{-3} to 14.1× 10^{-3} μF cm^{-2} whereas addition of halide ions to GAI caused subsequent decrease in C_{dl} up to 12.3× 10^{-3} μF cm^{-2} which increases the thickness of double layer. R_{ct} was maximum for 60 ppm GAI + 1 mM KI mixture. The order of inhibition performance was GAI + KI > GAI + KBr > GAI + KCl.

Scanning electron microscopy: Figs. 8(a)-8(f) show sthe SEM images of carbon steel coupons before and after immersion in sulphuric acid solution with and without GAI and GAI + halide mixture. Fig. 8(a) exemplifies the polished surface of the carbon steel specimen before immersion in the aggressive medium, while Fig. 8(b) represents the effect of 1 N H_2SO_4 solutions on the carbon steel specimen after 1 h immersion which clearly shows large rough pits and corrosion products due to acid attack. On assessing the Figs. 8(c-f) which represents the SEM images of carbon steel specimen in the presence of GAI and GAI-halide mixture, it can be seen that corrosive effect is greatly reduced because of the presence of GAI and inhibitor

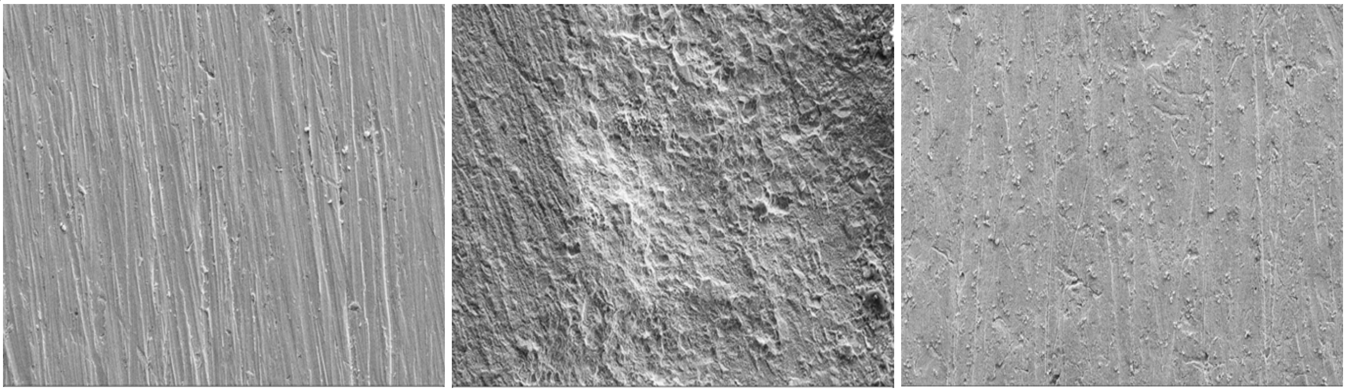

(a) Polished surface

(b) After immersion in 1 N H_2SO_4 solution

(c) in 60 ppm GAI

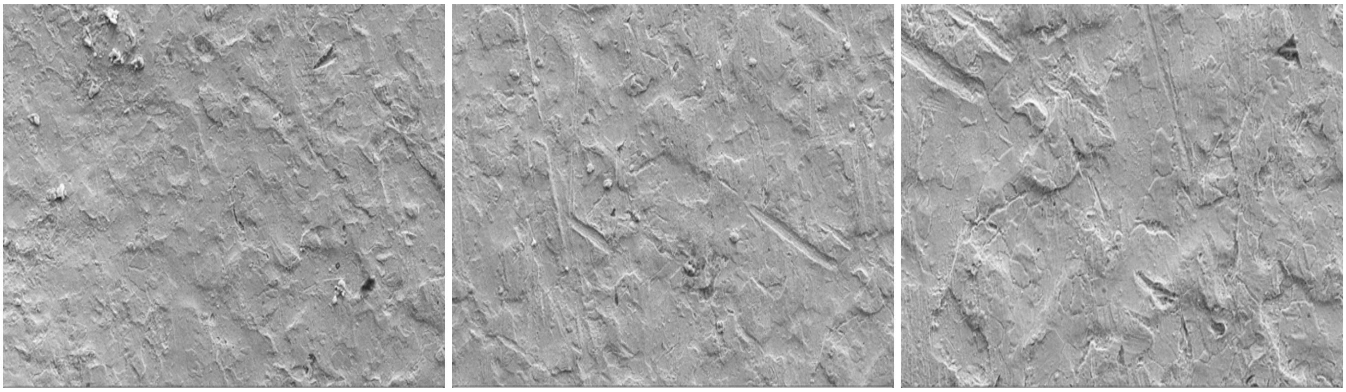

(d) in 60 ppm GAI and Cl^- mixture

(e) in 60 ppm GAI and Br^- mixture

(f) in 60 ppm GAI and I^- mixture

Fig. 8. SEM photographs of carbon steel sample

mixture adsorbed layer. Especially in presence of halide ions very compact, rough, porous, crack-free protective layer and products due to corrosion were produced over carbon steel substrate, which reduces the rate of corrosion to a greater extent. Thus GAI addition along with halide ions in aggressive medium has controlled the process of corrosion for carbon steel specimen in 1 N H_2SO_4 solution. The results obtained from the scanning electron micrographs are consistent with the fact that the mechanism of corrosion inhibition was adsorption.

Conclusion

- Synergistic influence of halides on GAI was found in the temperature range from 303 to 323 K for carbon steel in sulphuric acid.
- The performance order was observed as follows:

  GAI + KI > GAI + KBr > GAI + KCl
- Polarization measurements exhibit mixed type of inhibitor.
- Adsorption type is chemical at 1h and physical for 4 h immersion time.
- Adsorption mechanism was supported by SEM studies.

REFERENCES

1. D. Dwivedi, K. Lepkova and T. Becker, *RSC Adv.*, **7**, 4580 (2017); https://doi.org/10.1039/C6RA25094G.
2. S.A. Umoren, *Cellulose*, **15**, 751 (2008); https://doi.org/10.1007/s10570-008-9226-4.
3. A. Jano, A. Lame and E. Kokalari, *Kem. Ind..*, **61**, 497 (2012).
4. M. Abdallah, *Port. Electrochim. Acta*, **22**, 161 (2004); https://doi.org/10.4152/pea.200402161.
5. N.O. Eddy, S.E. Abechi, P. Ameh and E.E. Ebenso, *Walailak J. Sci. Technol.*, **10**, 247 (2013).
6. S.A. Umoren, I.B. Obot, E.E. Ebenso and N.O. Obi-Egbedi, *Desalination*, **247**, 561 (2009); https://doi.org/10.1016/j.desal.2008.09.005.
7. S.A. Umorena, I.B. Obota, E.E. Ebensob and N. Obi-Egbedi, *Port. Electrochim. Acta*, **26**, 199 (2008); https://doi.org/10.4152/pea.200802199.
8. P.O. Ameh, L. Magaji and T. Salihu, *Afr. J. Pure Appl. Chem.*, **6**, 100 (2012).
9. O.A. Paul, *Int. J. Phys. Sci.*, **9**, 184 (2014); https://doi.org/10.5897/IJPS2014.4116.
10. N.O. Eddy, P.O. Ameh and A.O. Odiongenyi, *Port. Electrochim. Acta*, **32**, 183 (2014); https://doi.org/10.4152/pea.201403183.
11. P.O. Ameh, A.O. Odiongenyi and N.O. Eddy, *Port. Electrochim. Acta*, **30**, 235 (2012); https://doi.org/10.4152/pea.201204235.
12. P.O. Ameh and N.O. Eddy, *Res. Chem. Intermed.*, **40**, 2641 (2014); https://doi.org/10.1007/s11164-013-1117-0.
13. N.O. Eddy, P.O. Ameh and E.E. Ebenso, *Int. J. Electrochem. Sci.*, **7**, 5677 (2012).
14. N.O. Eddy, P.O. Ameh, M.Y. Gwarzo, I.J. Okop and S.N. Dodo, *Port. Electrochim. Acta*, **31**, 79 (2013); https://doi.org/10.4152/pea.201302079.
15. N.O. Eddy, U.J. Ibok, P.O. Ameh, N.O. Alobi and M.M. Sambo, *Chem. Eng. Commun.*, **201**, 1360 (2014); https://doi.org/10.1080/00986445.2013.809000.
16. P.O. Ameh, *Int. J. Modern Chem.*, **2**, 28 (2012).
17. N.O. Eddy, P.O. Ameh, O.O. Anduang and V. Emaikwu, *Int. J. Chem. Mater. Environ. Res.*, **1**, 3 (2014).
18. N.O. Eddy, P.O. Ameh, O.O. Anduang and E.E. Ebenso, *Int. J. Electrochem. Sci.*, **7**, 7425 (2012).
19. Q. Qu, Z. Hao, S. Jiang, L. Li and W. Bai, *Mater. Corros.*, **59**, 883 (2008); https://doi.org/10.1002/maco.200804176.
20. N.O. Eddy, S.A. Odoemelam and A.O. Odiongenyi, *J. Appl. Electrochem.*, **39**, 849 (2009); https://doi.org/10.1007/s10800-008-9731-z.
21. S.A. Umoren, M.M. Solomon, I.I. Udosoro and A.P. Udoh, *Cellulose*, **17**, 635 (2010); https://doi.org/10.1007/s10570-010-9409-7.
22. M. Manickam, D. Sivakumar, B. Thirumalairaj and M. Jaganathan, *Adv. Phys. Chem.*, **Article ID 5987528** (2016); https://doi.org/10.1155/2016/5987528.
23. S. Mukherjee and H.C. Srivastava, *J. Am. Chem. Soc.*, **77**, 422 (1955); https://doi.org/10.1021/ja01607a059.
24. D.M.W. Anderson and A. Hendrie, *Carbohydr. Res.*, **20**, 259 (1971); https://doi.org/10.1016/S0008-6215(00)81379-8.
25. ASTM Practice Standard G-31, Standard Practice for Laboratory Immersion Corrosion Testing of Metals, ASTM International (2004).
26. K.O. Orubite and N.C. Oforka, *J. Mater. Lett.*, **58**, 1768 (2004); https://doi.org/10.1016/j.matlet.2003.11.030.
27. A.Y. El-Etre, *J. Appl. Surf. Sci.*, **252**, 8521 (2006); https://doi.org/10.1016/j.apsusc.2005.11.066.
28. E.E. Mola, *Electrochim. Acta*, **26**, 1209 (1981); https://doi.org/10.1016/0013-4686(81)85101-8.
29. M. Dahmani, A. Et-Touhami, S.S. Al-Deyab, B. Hammouti and A. Bouyanzer, *Int. J. Electrochem. Sci.*, **5**, 1060 (2010).
30. V. Ramesh Saliyan and A.V. Adhikari, *Bull. Mater. Sci.*, **31**, 699 (2007); https://doi.org/10.1007/s12034-008-0111-4.
31. L. Bammou, M. Belkhaouda, R. Salghi, O. Benali, A. Zarrouk, H. Zarrok and B. Hammouti, *J. Assoc. Arab. Univ. Basic Appl. Sci.*, **16**, 83 (2014); https://doi.org/10.1016/j.jaubas.2013.11.001.
32. M. Lebrini, F. Robert and C. Roos, *Int. J. Electrochem. Sci.*, **5**, 1698 (2010).
33. S.A. Ali, M.T. Saeed and S.U. Rahman, *Corros. Sci.*, **45**, 253 (2003); https://doi.org/10.1016/S0010-938X(02)00099-9.
34. E.E. Ebenso, *Mater. Chem. Phys.*, **79**, 58 (2003); https://doi.org/10.1016/S0254-0584(02)00446-7.
35. S.A. Umoren and U.F. Ekanem, *Chem. Eng. Commun.*, **197**, 1339 (2010); https://doi.org/10.1080/00986441003626086.
36. I.B. Obot, N.O. Obi-Egbedi and S.A. Umoren, *Corros. Sci.*, **51**, 276 (2009); https://doi.org/10.1016/j.corsci.2008.11.013.
37. G.N. Mu, X.M. Li and F. Li, *Mater. Chem. Phys.*, **86**, 59 (2004); https://doi.org/10.1016/j.matchemphys.2004.01.041.
38. X. Li, S. Deng, H. Fu and G. Mu, *Corros. Sci.*, **52**, 1167 (2010); https://doi.org/10.1016/j.corsci.2009.12.017.
39. S.A. Umoren, O. Ogbobe, I.O. Igwe and E.E. Ebenso, *Corros. Sci.*, **50**, 1998 (2008); https://doi.org/10.1016/j.corsci.2008.04.015.
40. A.G. Maitra Singh and B.B. Chakraborty, *Trans. Soc. Adv. Electrochem. Sci. Technol.*, **18**, 335 (1983).
41. A.I. Onuchukwu, S.P. Trasatti and S. Trasatti, *Corros. Sci.*, **36**, 1815 (1994); https://doi.org/10.1016/0010-938X(94)90020-5.
42. S.A. Umoren, Y. Li and F.H. Wang, *Corros. Sci.*, **52**, 2422 (2010); https://doi.org/10.1016/j.corsci.2010.03.021.
43. D.Q. Zhang, L.X. Gao and G.D. Zhou, *J. Appl. Electrochem.*, **33**, 361 (2003); https://doi.org/10.1023/A:1024403314993.
44. A.Y. Musa, A.B. Mohamad, A.A.H. Kadhum, M.S. Takriff and L.T. Tien, *Corros. Sci.*, **53**, 3672 (2011); https://doi.org/10.1016/j.corsci.2011.07.010.
45. D. Jayaperumal, *Mater. Chem. Phys.*, **119**, 478 (2010); https://doi.org/10.1016/j.matchemphys.2009.09.028.
46. E.S. Ferreira, C. Giacomelli, F.C. Giacomelli and A. Spinelli, *Mater. Chem. Phys.*, **83**, 129 (2004); https://doi.org/10.1016/j.matchemphys.2003.09.020.
47. N. Goudarzi, M. Peikari, M.R. Zahiri and H.R. Mousavi, *Arch. Metall. Mater.*, **57**, 845 (2012); https://doi.org/10.2478/v10172-012-0044-1.
48. G.T. Xavier, B. Thirumalairaj and M. Jaganathan, *Int. J. Corros.*, **Article ID 410120** (2015); https://doi.org/10.1155/2015/410120.
49. S.T. Arab and A.M. Al-Turkustani, *Port. Electrochim. Acta*, **24**, 53 (2006); https://doi.org/10.4152/pea.200601053.
50. I. Ahamad, R. Prasad and M.A. Quraishi, *Corros. Sci.*, **52**, 1472 (2010); https://doi.org/10.1016/j.corsci.2010.01.015.